# Size-Specific Interaction of Alkali Metal Ions in the Solvation of $M^+$−Benzene Clusters by Ar Atoms

**F. Huarte-Larrañaga,[†] A. Aguilar,[†,‡] J. M. Lucas,[†,‡] and M. Albertí*[,†,‡]**

*Centre especial de Recerca en Química Teòrica, Parc Científic de Barcelona, Josep Samitier 5, 08028 Barcelona, Spain, and Departament de Química Física i Centre especial de Recerca en Química Teòrica, Universitat de Barcelona, Martí i Franquès 1, 08028 Barcelona, Spain*

*Received: April 20, 2007; In Final Form: June 21, 2007*

The size-specific influence of the $M^+$ alkali ion (M = Li, Na, K, Rb, and Cs) in the solvation process of the $M^+$−benzene clusters by Ar atoms is investigated by means of molecular dynamic simulations. To fully understand the behavior observed in $M^+$−bz−$Ar_n$ clusters, solvation is also studied in clusters containing either $M^+$ or benzene only. The potential energy surfaces employed are based on a semiempirical bond-atom decomposition, which has been developed previously by some of the authors. The outcome of the dynamics is analyzed by employing radial distribution functions, studying the evolution of the distances between the Ar atoms and the alkali ion $M^+$ or the benzene molecule for all $M^+$−bz−$Ar_n$ clusters. For all members, in the $M^+$−bz series, the benzene molecule (bz) is found to remain strongly bound to $M^+$ even in the presence of solvent atoms. The radial distribution functions for the heavier clusters ($K^+$−bz, $Rb^+$−bz, and $Cs^+$−bz), are found to be different than for the lighter ($Na^+$−bz and $Li^+$−bz) ones.

## 1. Introduction

Solvation of ions is one of the most attractive fields of research in chemistry, mainly due to its fundamental role in a wide variety of chemical and biological systems.[1,2] The way in which the structure of the solvent is modified by the introduction of ions and how this determines the properties of the solution is a paradigmatic problem of electrochemistry. The solvation structure and dynamics of ions also plays an important role in many chemical and biochemical processes. Consequently, a great effort of experimental and theoretical research groups has been devoted to this subject since the early 1930s.[3,4] Besides, the interactions between cations and aromatic systems are greatly involved in many biological processes, such as molecular recognition and drug action.[5] Experimental and theoretical works have shown that the cation−$\pi$ interaction has a generally longer range than other nonbonding ones. Thus, the understanding of this interaction can help understand its crucial role in the design of new proteins or drugs. Most previous works on the cation−$\pi$ interaction have been carried out (either theoretical or experimental) in the gaseous phase. However, most of the chemical and biochemical processes of interest take place in solution and therefore the introduction of a solvent in both the theoretical simulations and experiments can be important. In spite of the great effort invested in the experimental characterization of solvation, the microscopic details of solvation of alkali cations still escape accurate experimental investigations. Molecular dynamics (MD) simulations can in principle fill the gap of the experimental limitations and thus provide an atomic perspective of the structure and dynamics of the solvation shell, which is regarded as a fundamental piece in view of the emerging field of nanobiotechnology. The experimental advances in generating van der Waals clusters has fostered theoretical studies on their structure and dynamical behavior.[6] In particular, the study of van der Waals clusters formed by a solute molecule embedded in a flexible cage of solvent atoms (or molecules) has been recognized as a powerful tool to investigate the process of solvation.[6,7] This is the case of aromatic molecule−rare gas complexes that can be viewed as a solute (aromatic) molecule in a well-characterized local solvent configuration (rare gas).[8,9] Solvation mechanisms in these systems can be related to both the existence of different minima in the potential energy surface (PES)[10] and the modification of different layers of solvent.[11] In these theoretical studies, the contribution of each microsolvation step can be identified and characterized. In particular, careful examination of the isomerization dynamics involving different minima helps to rationalize the structural behavior of these microsolvated clusters.[6,12] The inert gas atoms with their formally filled valence shell, can be considered as the simplest of solvents[6] and, thus, suitable prototypes for modeling solvents. In particular, Ar atoms are popular surrogates of water for molecular dynamics simulations, mainly because of their similar polarizability. Several studies can be found in the literature, in which aromatic compounds surrounded by Ar atoms are considered to rationalize aspects as structure, formation, and partition function[13−16] and microsolvation mechanisms.[11,17−19] Other studies, however, consider the benzene molecules to simulate the solvent effects.[20−23]

These studies, commonly performed for neutral systems, can be extended to ionic clusters which, in the presence of aromatic molecules, are mainly stabilized by cation−$\pi$ interaction. As already mentioned, this interaction is of great interest because it plays an important role in recognition processes in biological systems.[23−25] Among cations, the particular characteristics of both alkali and alkaline-earth cations make them good candidates for metal-centered clusters.[26] These ions, because of the relatively strong electrostatic interactions, are able to form

* Corresponding author. E-mail: m.alberti@ub.edu.
[†] Parc Científic de Barcelona.
[‡] Universitat de Barcelona.

10.1021/jp073063d CCC: $37.00 
Published on Web 07/28/2007

clusters with several polar species. Accordingly, the ions are good candidates to be used to analyze the competitive solvation by different partners.[20,21,27] Of particular interest is the size-selective nature of the cation$-\pi$ interaction, which study can be performed[23,25,28] by considering different members of the cations series.

The collective interactions that take place in ionic clusters are difficult to quantify at the ab initio level. The construction of suitable semiempirical PES models to describe the main features of ionic systems is therefore an important issue in the dynamic study of these systems. The proper representation of the interaction components together with the dynamics study has been the focus of our recent research and, in recent times, we have participated in the construction of force fields based on atom(ion)$-$bond interactions. This formulation of the interaction potential was initially applied to study neutral systems as, for example, bz$-$Ar$_n$ clusters.[15] Next, the formulation was extended to describe also ionic clusters containing benzene and alkaline ions, including an ion$-$quadrupole term to describe the whole interaction. The results for $M^+-$bz systems (M = Li, Na, K, Rb, Cs) have been tested by comparing our predictions with ab initio calculations. The agreement between predictions of the model and ab initio results was found to be very good.[29] The constructed force field was used to study the following systems: $K^+-$bz$-$Ar$_n$[30] and $Rb^+-$bz$-$Ar$_n$,[31] with $n$ ranging up to a maximum value of 3 Ar atoms. The formulation of the force field has also been tested for the anionic $Cl^--$bz system.[32] More complex systems such as $K^+-$(bz)$_2-$Ar$_n$ ($n = 1-3$)[33] and $Na^+-$bz$-$Ar$_n$ ($n = 1-19$) systems[12] have also been investigated. Molecular dynamics simulations have shown specific trends of the solvation mechanism for $K^+-$(bz)$_2-$Ar$_n$[33] and $Na^+-$bz$-$Ar$_n$ systems[12] as the number of solvent atoms increases. The dynamical study of the $K^+-$(bz)$_2-$Ar$_n$ system showed that Ar atoms tend to be placed near the cation, entering in the $K^+-$(bz)$_2$ sandwich system and deforming it into a V-shape, thus allowing a more direct contact between Ar and $K^+$. The dynamical study of $Na^+-$bz$-$Ar$_n$ showed that a sufficient increase of the number of Ar atoms tends to create multiple layers around the solute (microsolvation process).

In the work presented here, we focus our attention on the behavior of the $M^+-$bz series of clusters solvated by Ar atoms, with $M^+$ being an alkali ion, and consider the cation-size-specific influence. The time averaged distribution of Ar atoms around the cations will be given and compared with the corresponding distributions for bz$-$Ar$_n$ and $M^+-$Ar$_n$ systems. The paper is articulated as follows: in the next section an outline of the construction of the potential energy surfaces employed is given. Then, results provided by the dynamics simulation of the solvation process are reported in section 3. To better understand the solvation in $M^+-$bz clusters (section 3.3), we have also included results for $M^+-$Ar$_n$ (section 3.1) and benzene$-$Ar$_n$ clusters (section 3.2). Our main conclusions are finally presented in section 4.

## 2. Potential Energy Surfaces

Considering that bound clusters are mainly dominated by pairwise additive two-body forces,[8] the approximation most often used in the construction of potential energy functions (to be used later in dynamic simulations) is to describe the noncovalent interactions as a pairwise summation of atom$-$atom model potentials.[34] However, the need for including contributions other than the pure atom$-$atom ones has been repeatedly discussed in the literature.[11,17−19]

In recent times, we have collaborated in the development of an alternative representation of the force field, which incorporates some of the many-body effects, without losing the advantage of formulating the interaction as a sum of two-body-like terms. In this model, the nonelectrostatic contribution to the atom (ion)$-$molecule interaction is described by means of a sum of atom (ion)$-$bond functions. The potential energy surface (PES) model has been described in detail previously,[30,32] and here only a brief description of the interaction potential will be given.

For neutral clusters, as for instance the Ar$-$bz system, the interaction potential is described through the sum of twelve atom-bond interaction terms. Whenever the neutral atom is replaced by an ion ($M^+-$bz clusters), an additional contribution (the electrostatic one), reflecting the ion-quadrupole interaction, needs to be considered. In this case, the total potential interaction, $V_{\text{total}}$, is expressed as the sum of an electrostatic ($V_{\text{el}}$) and a nonelectrostatic ($V_{\text{nel}}$) term. For more complex clusters, as for instance $M^+-$bz$-$Ar$_n$, the $M^+-$Ar and Ar$-$Ar interactions need to be considered as well.

Accordingly, for $M^+-$benzene$-$Ar$_n$ clusters, $V_{\text{nel}}$ has the following form

$$V_{\text{nel}} = \sum_{i=1}^{6}(V_{M^+-(CC)_i} + V_{M^+-(CH)_i}) + \sum_{j=1}^{n}\sum_{i=1}^{6}(V_{Ar_j-(CC)_i} + V_{Ar_j-(CH)_i}) + \sum_{j=1}^{n}V_{M^+-Ar_j} + \sum_{j=1}^{n-1}\sum_{k=j+1}^{n}V_{Ar_j-Ar_k} \quad (1)$$

where each atom(ion)-bond term is expressed as follows

$$V(r,\alpha) = \epsilon(\alpha)\left[\frac{m}{n(r,\alpha)-m}\left(\frac{r_0(\alpha)}{r}\right)^{n(r,\alpha)} - \frac{n(r,\alpha)}{n(r,\alpha)-m}\left(\frac{r_0(\alpha)}{r}\right)^{m}\right] \quad (2)$$

where $r$ is the distance of the atom (or the ion) to the middle of the considered bond and $\alpha$ is the angle formed by the bond and $r$. The parameter $m$ is taken equal to 6 for atom$-$bond interactions and 4 for ion$-$bond ones. The parameters $\epsilon$ and $r_0$, representing the depth of the potential well and its location respectively, are expressed as a function of $\alpha$ in terms of their parallel ($\epsilon_{\|}$ and $r_{0\|}$) and perpendicular ($\epsilon_{\perp}$ and $r_{0\perp}$) values using simple trigonometric formulas.[30] These are derived from the charge and the polarizability of the related atomic species as well as polarizability and effective polarizability tensor components of aromatic CC and CH bonds. The parameter $n$ is also expressed as a function of both $\alpha$ and $r$,[15]

$$n(r,\alpha) = \beta + 4.0\left(\frac{r}{r_0(\alpha)}\right)^2 \quad (3)$$

with the $\beta$ parameter being set, in our case, equal to 10.0.

The $M^+-$Ar and Ar$-$Ar interactions are formulated similarly to eq 2 but removing the angular dependence.

On the other hand, $V_{\text{el}}$ is calculated by means of the following equation

$$V_{\text{el}} = \sum_{i=1}^{18}\frac{q_{M^+}q_i}{4\pi\epsilon_0 r_{M^+-q_i}} \quad (4)$$

where the sum is over 18 charges, 6 of +0.092 45 au on each H atom and 12 negative charges of −0.046 23 au placed on the C atoms of benzene on both sides of aromatic ring. This charge distribution for the benzene molecule ensures the reproduction of its quadrupolar moment.

**TABLE 1: Ar−Ar and $M^+$−Ar Parameters for $M^+$−bz−$Ar_n$ Clusters.**

| pair | $\epsilon$/meV | $r_0$/Å | $m$ |
|---|---|---|---|
| Ar−Ar | 12.34 | 3.76 | 6 |
| $Li^+$−Ar | 254 | 2.42 | 4 |
| $Na^+$−Ar | 167 | 2.73 | 4 |
| $K^+$−Ar | 110 | 3.19 | 4 |
| $Rb^+$−Ar | 97 | 3.36 | 4 |
| $Cs^+$−Ar | 85 | 3.57 | 4 |

The $\epsilon_{||}$, $r_{0||}$, $\epsilon_{\perp}$, and $r_{0\perp}$ parameters for Ar−bz and $M^+$−Ar systems are given in refs 16 and 32, respectively. In Table 1 the relevant parameters to describe the Ar−Ar and $M^+$−Ar interactions are listed.

This formulation of the potential energy allows us to interpret the results obtained from dynamics simulations in terms of the different contributions to the total energy.

The large number of degrees of freedom of this type of clusters leads to quite structured PESs. As the number of Ar solvents increases, the number of different configurations of these clusters that are stabilized by a corresponding well on the PES also increases.

## 3. Dynamic Simulations

The dynamics of the clusters has been investigated by considering a microcanonical ensemble (NVE) of atoms and treating the benzene molecule as a rigid body. The molecular simulations at the different energy conditions have been performed looping over increasing values of the total energy ($E_{total}$) using the DL_POLY suite of codes.[35] The range of the total energies investigated corresponds to a temperature range of $T \in [2-100]$ K, where $T$ is the mean value of the temperature along the trajectory. Here, only results corresponding to $T =$ 25 K are given. These are representative of the investigated temperature range. The interaction energy for all atom−bond and atom−atom pairs was calculated at every step of the dynamics without imposing any cutoff radius. A time step of 1 fs has been used to integrate the dynamic equations, to keep the relative rms fluctuations of $E_{total}$ smaller than $10^{-5}$. The simulation time was set at 25 ns, this time being large enough to ensure that the mean values of the several energy contributions and temperature, $T$, do not vary when extending the calculations to longer times.

In particular, we are interested in the dynamic and static changes of the $M^+$−bz cluster solvation shell as more solvent atoms are included. To rationalize better the outcome of the dynamics, the results have been interpreted by comparison with those for the solvation of both the benzene molecule and the alkaline cations forming, respectively, $M^+$−$Ar_n$ and bz−$Ar_n$ clusters, similarly to what was done previously for the $Na^+$−bz−$Ar_n$ cluster.[12]

The study of the solvation process has been made by analyzing the radial distribution functions (rdf) of the Ar atoms around $M^+$, benzene, and the $M^+$−bz cluster. These functions have been calculated using

$$\mathrm{rdf} = 4\pi \sum_{i=1}^{n} r_i^2 P(r_i) \qquad (5)$$

where $r_i$ corresponds to the distance of the Ar atoms either to the cation or to the center of mass (c.o.m.) of benzene, represented in the graphics by $r(M^+-Ar_i)$ and $R$, respectively. $P(r_i)$ is the probability to find the Argon atom "$i$" at $r_i$ during the dynamics.

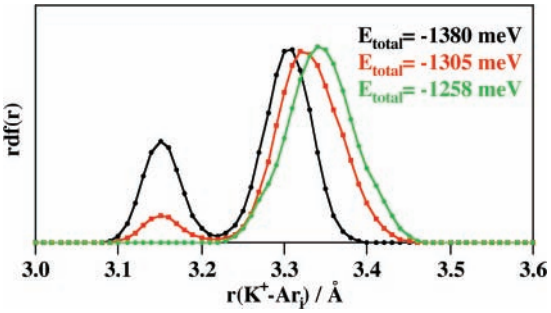


**Figure 1.** Radial distribution functions for the $K^+-Ar_{10}$ cluster.

The PESs describing the solvated $M^+$−bz ($M^+$−bz−$Ar_n$) clusters, present several stable configurations which, depending on the ion $M^+$ size, can give rise to interconversions and thus isomerization processes, even at not very high temperatures. However, those clusters having a more compacted structure, as is the case of clusters with the first solvation shell completed, the isomerization process needs higher temperature values to take place, as will be discussed later.

At this point, it should be mentioned that as more Ar atoms are included in the simulation, the "additional" atoms tend to be placed either in the less favorable positions on the same side of the benzene plane as the cation or on the opposite side of the benzene plane. Both situations favor complicated isomerization processes, which make it difficult to analyze changes in the distibution of Ar atoms around the cluster in terms of the cluster size. When the isomerization process takes place, the rdfs become highly structured and difficult to be interpreted. Accordingly, to avoid as much as possible very complex isomerization processes, the rdf analysis for $M^+$−bz−$Ar_n$ clusters has been made by considering a maximum of nine Ar atoms, all of them placed initially on the same side of the benzene plane as the cation. A larger number of Ar atoms has been, however, included in the $M^+$−$Ar_n$ dynamics simulations.

**3.1. Solvation of $M^+$ Ions.** As indicated in the previous section, the potential energy for $M^+$−$Ar_n$ clusters is described by means of a sum of all pair potentials, $n$ pairs describing the interaction between Ar and $M^+$, and $n(n-1)/2$ pairs describing the interaction between two Ar atoms. As evidenced in Table 1, the largest interaction is found for the lightest ion and the minimum of the $M^+$−Ar potential well is placed at increasing distances as the ion mass increases. This means that to analyze the solvation of $M^+$ ions, two aspects need to be considered: the equilibrium distance for $M^+$−Ar systems ($r_0$ column in Table 1) and the magnitude of the interaction energy ($\epsilon$ in Table 1). The first aspect causes the heavier ions to have a larger $M^+$−Ar equilibrium distance and thus more Ar atoms are needed to complete the first solvation shell (static point of view), whereas the second one can be related to the fluidity of the motion of the Ar atoms around the $M^+$ cation (dynamic point of view). In fact, for simulations performed at low values of $E_{total}$ the solvent atoms remain close to their equilibrium positions. These positions are more "fixed" for the lighter cations (where $\epsilon$ is larger) and rather "loose" for the heavier ones. However, at increasing values of $E_{total}$ the Ar atoms can move easily along the dynamics simulation, occupying positions far away from the equilibrium ones. This is the case of $M^+$−$Ar_n$ clusters, where the first solvation shell is not yet complete, and especially for those clusters involving a heavy cation.

If one bears in mind that the interaction energy is smaller for Ar−Ar than for $M^+$−Ar, one should not be surprised to find Ar atoms distributed around the ion. In fact, the simulations evidence that the Ar atoms tend to place themselves sym-

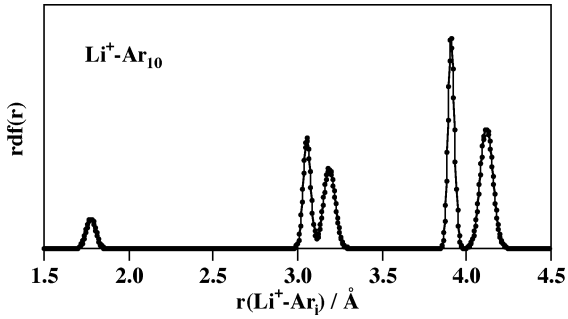


**Figure 2.** Radial distribution function for the $Li^+-Ar_{10}$ cluster.

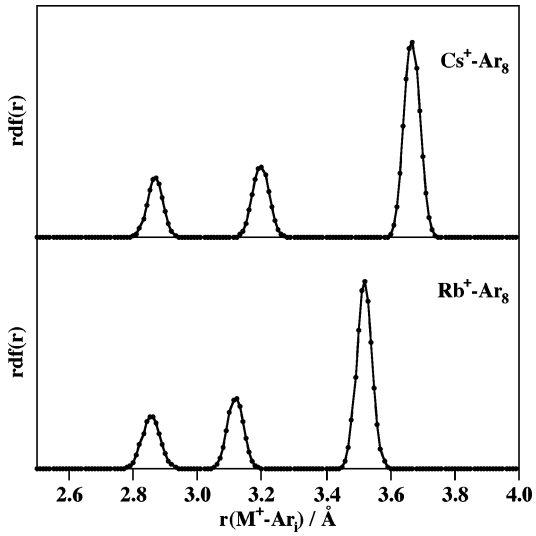


**Figure 3.** Radial distribution functions for the $Rb^+-Ar_8$ (lower panel) and $Cs^+-Ar_8$ (upper panel) clusters.

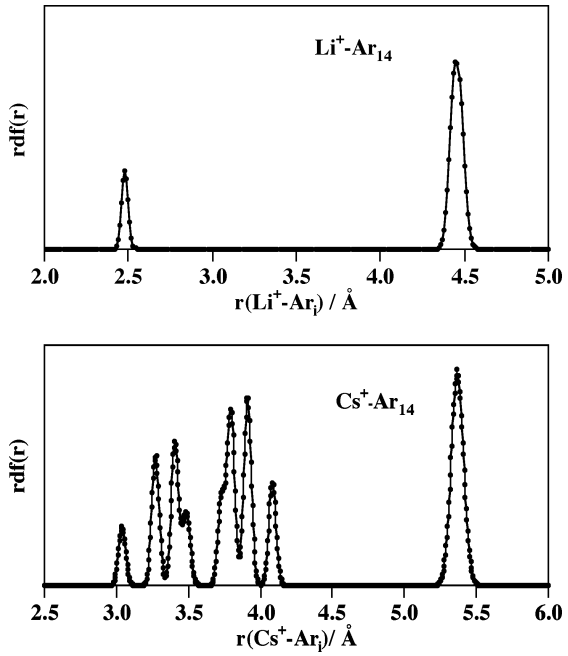


**Figure 4.** Radial distribution functions for the $Li^+-Ar_{14}$ (lower panel) and $Cs^+-Ar_{14}$ (upper panel) clusters.

metrically around the cation. This can be analyzed from the radial distribution functions plotted as a function of the distance of the Ar atoms to the corresponding cation. The rdfs corresponding to clusters with a few Ar atoms (their number depending on the cation mass) show only one peak. For a larger number of Ar atoms, these can no longer be distributed in the first solvation shell near the cation and other less favorable positions in the second solvation shell will be occupied and a second peak (structure) will appear in the rdfs. Thus, rdfs with only one maximum should generally indicate the completeness of the first solvation shell. However, one must also consider that rdfs can show only one peak under certain circumstances, even if the first solvation shell is incomplete. For instance, this is the case of some solvated cluster dynamic simulations performed at low energies (starting from an initial configuration of the cluster close to the equilibrium one), reflecting the static properties of the system. This has been observed in our previous study of the solvation of $Na^+-$bz with Ar atoms.[12] On the other hand, if the energy of the molecular dynamics trajectory $E_{total}$ is increased, the Ar atoms can explore more repulsive zones of the potential energy surface and then the corresponding rdf should look quite different. One can thus conclude that whenever the first solvation shell is not full, the form of the rdfs depends on the initial conditions of the simulation.

The presence of various peaks in the rdf can thus be associated either with the presence of some of the solvent atoms in the second solvation shell or with the movement of the first solvation shell Ar atoms around the cation because it is not complete. In the first case, the peaks are all around the main first solvation shell peak, whereas in the second case they are spread along a wide radius range.

Now that the general trends of the $M^+-$Ar cluster rdfs have been discussed, we proceed to a more detailed discussion of the particular rdfs given for each of the ions in the series.

In Figure 1 three rdfs for the $K^+-Ar_{10}$ system are shown, corresponding to molecular simulations carried out at three different total energies. According to our dynamics simulations, the $K^+$ ion needs 12 Ar atoms to complete the first solvation shell. The rdf with one single peak (green color), has a maximum at a larger distance than the maxima of the other two curves. In the same figure it can be appreciated that for those rdfs with more than one peak, both maxima are separated by short distances (about 0.2 Å), thus reflecting the dynamic fluctuations due to the incompleteness of the first solvation shell.

Performing numerous dynamics simulations for the different alkali ions and adding Ar atoms, we have observed that the first solvation shell around the lightest $Li^+$ cation is completed with 6 Ar atoms, whereas 10 Ar atoms are needed to complete the first solvation shell for $Na^+$ and 12 for the remaining cations. Considering this, it is not surprising that the rdf for the $Li^+-Ar_{10}$ cluster shown in Figure 2 looks very different than that for the $K^+-Ar_{10}$ cluster (Figure 1). As can be seen in the figure, the rdf for $Li^+-Ar_{10}$ is much more structured than for $K^+-Ar_{10}$. The rdf for the $Li^+-Ar_{10}$ cluster has some peaks close to one another (~0.2 Å), reflecting the motion of the solvent atoms on the same solvation shell. Besides these peaks, some other peaks are separated by larger distances; these are due to the presence of some Ar atoms in the second solvation shell. A rather small peak can also be seen in the rdf of Figure 2, at distances between 1.5 and 2.0 Å. This is probably due to the interaction between solvent atoms, which causes some Ar atom to occupy a much closer position for a short time.

The systematic study of the solvation of the different alkaline ions by Ar atoms shows that the distance between peaks, associated with Ar atoms placed either on the same or on different solvation shells, increases with the ion size. This behavior can be seen in Figure 3 where rdfs for $Rb^+-Ar_8$ and $Cs^+-Ar_8$ systems are presented.

At a given total energy, the structure of the rdf depends on the compactness of the cluster. A rdf with a small number of

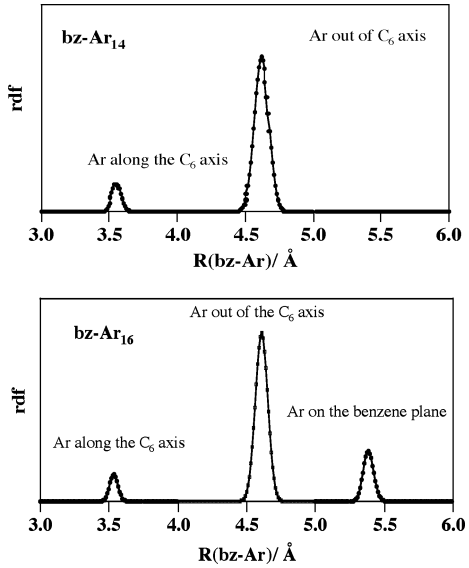


**Figure 5.** Radial distribution functions for the bz−$Ar_{14}$ and bz−$Ar_{16}$ clusters referred to the distance of Ar atoms to the center of mass of benzene.

peaks should indicate a rather compact solvation shell, but a diffuse or labile solvation shell will correspond to a very structured rdf. In Figure 4 the results for the lightest and the heaviest $M^+-A_{14}$ clusters are compared. For instance, the lighter $Li^+-Ar_n$ systems, for which the first solvation shell is completed with 6 Ar atoms, needs 8 additional Ar atoms to complete the second solvation shell. Accordingly, the $Li^+-Ar_{14}$ cluster shows a highly compacted structure, and the corresponding rdf shows only two peaks (see Figure 4, upper panel). On the contrary, the remaining heavier alkaline ions for which the first solvation shell is completed with 10 ($Na^+$) and 12 ($K^+$, $Rb^+$ and $Cs^+$) Ar atoms, form $M^+-Ar_{14}$ clusters, which do not present such a compacted structure because of the incompleteness of the second solvation shell and, as a result, the corresponding rdfs are much more structured than for $Li^+-Ar_{14}$.

**3.2. Solvation of Benzene.** The solvation of benzene has been analyzed in detail in ref 12 and here only some necessary details are given. To understand better the distribution of Ar atoms in the cluster, the rdfs for the bz−$Ar_{14}$ and the bz−$Ar_{16}$ clusters are given in Figure 5. As shown in ref 12, the first two Ar atoms solvating the benzene molecule tend to be placed along the $C_6$ symmetry axis on both sides of the aromatic ring. As the number of solvent atoms is increased, the additional Ar atoms are distributed symmetrically around the $C_6$ symmetry axis until the first solvation shell is complete. For instance, the most stable configuration for the bz−$Ar_{14}$ cluster is the one with six Ar atoms forming a hexagonal umbrella around the symmetry axis on both sides of the aromatic ring. Accordingly, the corresponding rdf shows two peaks, as can be seen in the upper panel of Figure 5. The first peak is associated with the position of two atoms along the $C_6$ axis, and the second one reflects the distribution of the remaining 12 atoms wrapping the aromatic ring. These peaks are found at distances of about 3.5 and 4.7 Å to the c.o.m. of benzene, respectively. The first of them, peaking at short distances, corresponds to a distance very similar to that of Ar at the equilibrium geometry in the bz−Ar system.[15] Although six other equivalent on-plane wells exist for the bz−Ar system, the remaining 12 Ar atoms tend to occupy out-of-plane positions. Accordingly, the second peak appears at shorter distances than the one corresponding to the on-plane minima (5.3 Å). When the number of Ar atoms is large enough and the most favorable positions are full, some of the Ar atoms tend to occupy positions near the plane of the benzene (bridging atoms). The bridge atoms tend to be all at the same distance from the c.o.m. of benzene, and consequently, a third peak appears for a benzene cluster with more than 14 Ar atoms. See, for instance, the third peak at a distance of 5.4 Å for the bz−$Ar_{16}$ cluster (lower panel, Figure 5). A further increase in the number of solvents gives more bridging atoms in the cluster, but the form of the rdf remains nearly unchanged until the first solvation shell is full.

**3.3. Solvation of $M^+$−Benzene.** Finally, we consider the simulations performed for $M^+-bz-Ar_n$ clusters. Due to the different magnitudes of the contributions to the interaction energy in these clusters, the benzene molecule remains strongly bound to $M^+$ and Ar atoms stay preferentially close the cation. The spatial distribution of Ar atoms around $M^+$−bz clusters is then less symmetric than the corresponding distributions in $M^+-Ar_n$ or benzene−$Ar_n$ clusters. When this type of rearrangement occurs, rdf plots become more structured. In this case, it is of some help to divide the first solvation shell into two-half-sells,

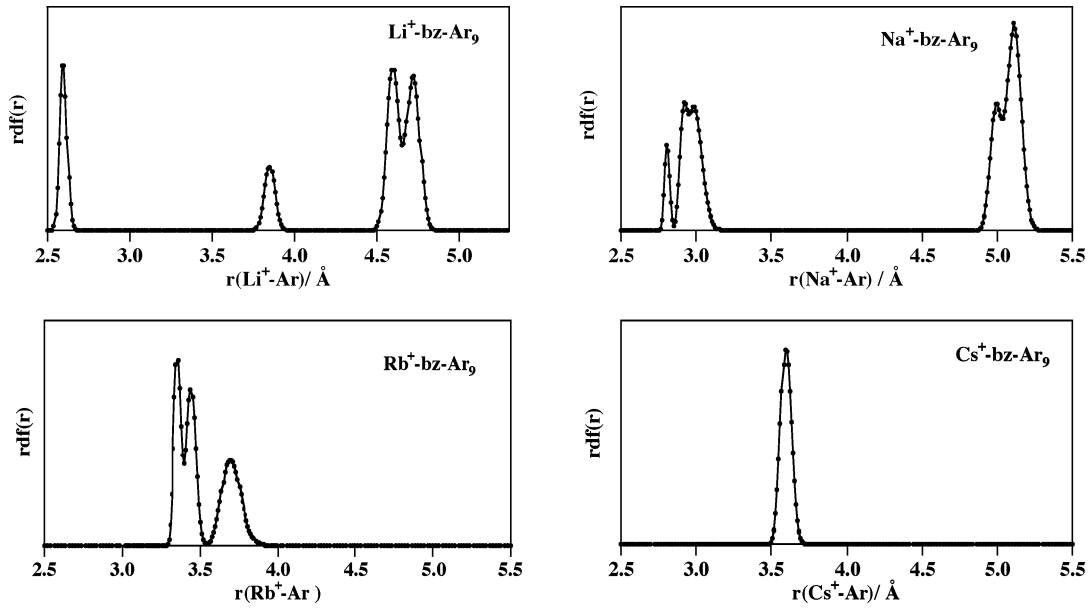


**Figure 6.** Radial distribution functions for the $M^+-bz-Ar_9$ (M = Na, K, Rb, Cs) as a function of the distance of Ar atoms from $M^+$.

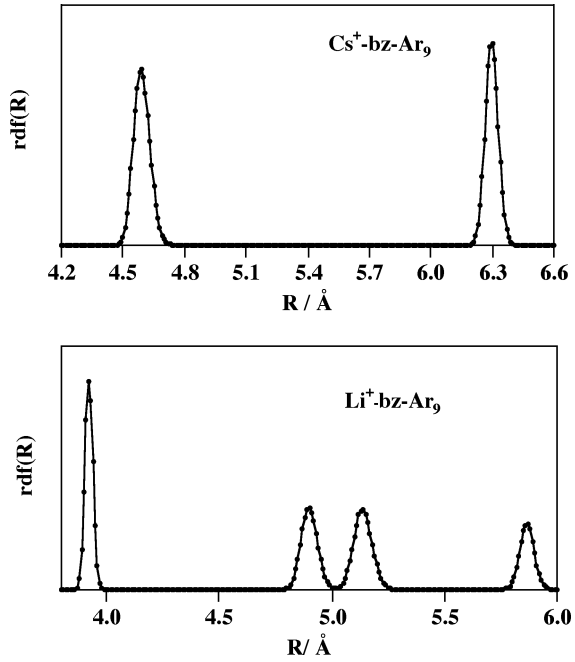


**Figure 7.** Radial distribution functions for the $Li^+-bz-Ar_9$ (lower panel) and $Cs^+-bz-Ar_9$ (upper panel) clusters referred to the center of mass of benzene.

one on the same side of the benzene plane as the cation and the other one on the opposite side, separated by the aromatic ring.

Results of ab initio calculations carried out for the $M^+-bz$ family of clusters show that the interaction energy decreases and the equilibrium distance of $M^+$ to the c.o.m. of benzene increases as the mass of the cation is increased.[27] According to this, heavier clusters need more Ar atoms than the lighter ones to complete the first solvation half-shell on the same side of the benzene plane as the cation. Results show that some of the Ar atoms solvating the cluster are placed in the energetically most favorable positions, interacting with both benzene and the cation. Moreover, the solvent atoms tend to be placed preferably out of the benzene plane, being distributed, as close as possible to the cation. When $R(M^+-bz)$ increases to large enough distances, Ar atoms can be placed above and below the cation (close to the benzene). However, for the lightest cluster, positions between benzene and the cation are quite unlikely for solvent atoms.

In the absence of other molecules, benzene remains always strongly bound to the cation. By regarding the overall process as a competitive solvation of $M^+$ by benzene and Ar atoms, the benzene molecule is always placed in the first layer of solvation around the cation for all $M^+-bz-Ar_n$ clusters.

As a representative example to study the particularities of the solvation process, the $M^+-bz-Ar_9$ clusters have been considered. In Table 2, the corresponding mean values of the different energy contributions found at low temperatures for the $M^+-bz-Ar_9$ cluster family are listed. In this table, $E_{cfg}$ represents the potential energy of the cluster resulting from the following contributions: the electrostatic and van der Waals interactions between benzene and the cation ($E_{el}$ and $E_{M^+-bz}$, respectively), the interaction between benzene and Ar ($E_{Ar-bz}$), and the $M^+-$Ar and Ar$-$Ar interactions ($E_{bnd}$). As shown in the table, the highest contribution corresponds to $E_{bnd}$, and the lowest one is for the Ar$-$benzene interaction. Moreover, it can be observed that the relative contribution of $E_{bnd}$ increases with the size of the ion.

Figure 6 shows the rdfs for $M^+-bz-Ar_9$ (M = Li, Na, Rb, Cs) clusters represented as a function of the distance of the Ar atoms to the cation. The corresponding rdf for the $K^+-bz-Ar_9$ cluster is similar to the $Rb^+-bz-Ar_9$ cluster one and therefore it is not shown. All these results correspond to dynamical simulations in which the initial configuration of the cluster is one with all Ar atoms placed on the same side of the benzene plane as the cation. For $n = 1-9$, the Ar atoms stay preferentially close to the $M^+$ cation. If the simulation is started from a configuration in which Ar atoms are placed on both sides of the aromatic ring, then the interconversions of the solvent atoms give rise to noisy or nonrepresentative rdfs. Accordingly, it seems that a better understanding of the spatial ordenation should be achieved by considering as an initial configuration one with all Ar atoms are placed near the cation, on the same side of the aromatic ring.

As evidenced in the figure, the three peaks observed for the lightest cluster ($Li^+-bz-Ar_9$) tend to approach each other as the mass of the cation increases. In fact, in the case of the $Na^+-bz-Ar_9$ cluster, six of the nine Ar atoms tend to be placed at distances of about the equilibrium one for the $Na^+-$Ar (2.73 Å) system whereas the remaining three atoms are found at larger distances. The distance between the two groups of Ar atoms decreases with the size of the cation. In the case of the heavier clusters, the two groups of peaks are within a similar distance range, at an $R$ value of about the equilibrium distance for the $M^+-$Ar system. For instance, in the case of the $Cs^+-$Ar system the equilibrium distance is 3.57 Å and in Figure 6 it can be seen that the rdf peaks at a value near 3.5 Å. The transition from three peaks to one peak in the rdf when going from the $Li^+-bz-Ar_9$ cluster to the $Cs^+-bz-Ar_9$ one can be explained from energetic and geometrical considerations.

In Figure 7 the rdfs referred to the benzene center of mass are shown for the heaviest and lightest cation clusters, solvated by nine Ar atoms.

In fact, the rdfs are the footprint of the equilibrium geometries for these clusters, as can be seen in Figure 8. In the upper panel of the figure is represented the preferred distribution of nine Ar atoms around the $Cs^+-bz$ cluster, and the same representation for the $Li^+-bz$ cluster is shown in the lower panel of Figure 8. In the case of the lighter cluster, due to the magnitude of the several contributions to the interaction, the Ar atoms can get closer to both bz and $Li^+$. The solvent atoms feel strongly the interaction with both the cation and the benzene molecule, which are quite close to one another. Thus the solvent atoms occupy positions with a rather open angle with respect to the benzene symmetry axis. The Ar atoms can then be grouped in sets of four atoms forming a more or less regular square, parallel to the benzene plane. A first group occupying nearly bridge (on plane) position corresponds to the doublet at 5 Å in Figure 7 (lower panel). A second group of Ar atoms also forms a less

**TABLE 2: Contributions to the Configuration Energy, $E_{cfg}$, for $M^+-bz-Ar_9$ Clusters**

| $M^+-bz-Ar_9$ | $T$/K | $E_{cfg}$/meV | $E_{el}$/meV | $E_{M^+-bz}$/meV | $E_{Ar-bz}$/meV | $E_{bnd}$/meV |
|---|---|---|---|---|---|---|
| $Li^+-bz-Ar_9$ | 2.9 | −2997 | −997 | −651 | −163 | −1186 |
| $Na^+-bz-Ar_9$ | 2.1 | −2507 | −808 | −435 | −193 | −1071 |
| $K^+-bz-Ar_9$ | 2.6 | −2141 | −618 | −305 | −167 | −1051 |
| $Rb^+-bz-Ar_9$ | 3.0 | −2018 | −558 | −268 | −161 | −1031 |
| $Cs^+-bz-Ar_9$ | 3.3 | −1859 | −494 | −231 | −171 | −963 |

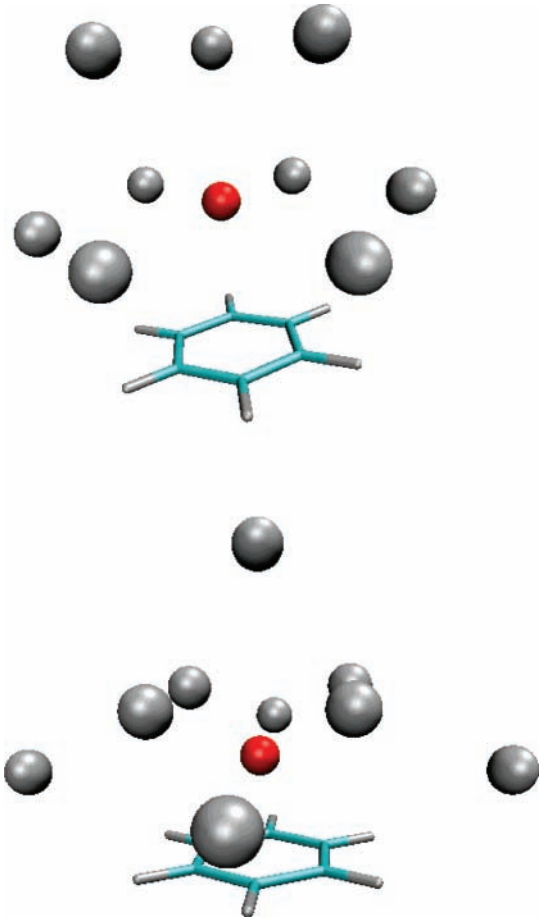

**Figure 8.** Equilibrium geometry for $Li^+-bz-Ar_9$ (lower panel) and $Cs^+-bz-Ar_9$ (upper panel) clusters.

regular square corresponding to the first peak at about 4 Å. The last solvent atom, located on the benzene $C_6$ symmetry axis (peak at ~5.9 Å) experiences the interaction with the $Li^+$ cation and the four Ar atoms that are closer. In the case of the heavier $Cs^+-bz$ cluster, the solvent atoms are farther apart from the benzene molecule. Then, the first six Ar atoms form a rather regular hexagon (first peak at ~4.5 Å, upper panel in Figure 7) and the remaining three atoms for a plane parallel to the first one (peak at ~6.3 Å). In this case, no Ar atoms are placed in the symmetry axis. The main difference between the two clusters is the distance between the two planes of Ar atoms (almost parallel to benzene) and the distance between the cation and the Ar atoms (consequence of the different interaction energy).

The equilibrium geometry of the remaining $M^+-bz-Ar_9$ clusters is similar to that of $Cs^+-bz-Ar_9$. In general, the clusters show equilibrium geometry configurations (without bridge atoms) where all Ar atoms tend to solvate the cation.

By increasing the number of Ar atoms, the preference to solvate $M^+$ better than the benzene has been observed together with the existence of different microenvironments associated with the structure of the minima occurring on the potential energy surface.

As indicated in ref 12, the different contributions from the various potential energy terms originates some particular effects when the number of solvents increases (for instance, the interaction energy between $Na^+$ and Ar at the equilibrium distance is nearly the same as that for the $bz-Ar_{14}$ cluster). This means that the successive addition of solvent atoms tends to vary the position of the first ones. This behavior has been observed for all alkaline series of $M^+-bz$ clusters.

## 4. Conclusions

Solvation effects on $M^+-bz$ clusters have been investigated by employing Ar atoms as a solvent. A maximum of 19 solvent atoms have been included in our molecular dynamics simulations in the case of $M^+-Ar_n$ clusters. The microscopic solvation phenomena, clearly manifested by the existence of several microenvironments corresponding to different minima in the potential energy surface, have been investigated. To better understand these phenomena, the interpretation of the $M^+-bz-Ar_n$ dynamical results has been complemented with the dynamical study of the $M^+-Ar_n$ and $bz-Ar_n$ related clusters.

For all alkaline series of $M^+-bz$ clusters, it has been found that the successive addition of solvent atoms tends to vary the position of the first ones. This makes the identification of each individual contribution to the averaged results very difficult. In this line, the comparison between the solvation of the cations ($M^+-Ar_n$ clusters), benzene ($bz-Ar_n$ clusters), and $M^+-bz$ ($M^+-bz-Ar_n$ clusters) helps to interpret the solvation results. In particular, the radial distribution functions have proved useful to investigate the dynamics of the microsolvation. For $bz-Ar_n$ and $M^+-bz-Ar_n$ clusters, several stable configurations exist, with solvent atoms on one side and on both sides of the aromatic ring. The preference of Ar atoms to solvate $M^+$ better than benzene has been observed by increasing the number of solvent atoms. However, in the absence of other molecules, benzene remains always strongly bound to the cation. By regarding the overall process as a competitive solvation of $M^+$ by benzene and Ar atoms, the benzene molecule is always placed in the first layer of solvation around the cation for all $M^+-bz-Ar_n$ clusters. When the first shell of solvation is complete, the first "new" solvents prefer to occupy positions on the second solvation shell but closer to the cation than to benzene.

**Acknowledgment.** We acknowledge financial support from the Spanish DGICYT (Project CTQ2004-01102), MEC (Project UNBA05-33-001, CTQ2005-03721), DURSI (Project 2005 PEIR 0051/69). Also, thanks are due to the Centre de Supercomputació de Catalunya CESCA-C[4] and Fundació Catalana per a la Recerca for the allocated supercomputing time. F.H-L. acknowledges the Spanish Ministerio de Educación y Ciencia for a "Ramón y Cajal" fellowship.

## References and Notes

(1) Otashi, H.; Radnai, T. *Chem. Rev*. **1993**, *93*, 1157.
(2) Impey, R. W.; Madden, P. A.; McDonald, I. R. *J. Phys. Chem.* **1983**, *87*, 5071.
(3) *Ionic Hydration in Chemistry and Biophysics*; Studies in Physical and Theoretical Chemistry 12; Conway, B. E., Ed.; Elsevier: Amsterdam, 1981.
(4) *Ion solvation*; Marcus, Y., Ed.; Wiley: Chischester, U. K., 1986.
(5) Sa, R.; Zhu, W.; Shen, J.; Gong, Z.; Cheng, J.; Chen, K.; Jiang, H. *J. Phys. Chem. B* **2006**, *110*, 5094.
(6) Douin, S.; Parneix, P.; Amar, F. G.; Bréchignac, Ph. *J. Phys. Chem. A* **1997**, *101*, 122.
(7) Amirav, A.; Even, U.; Jortner, J. *J. Chem. Phys.* **1981**, *75*, 2489.
(8) Leutwyler, S.; Jortner, J. *J. Phys. Chem.* **1987**, *91*, 5558.
(9) Leutwyler, S.; Bösiger, J. *Chem. Rev*. **1990**, *90*, 489.
(10) Heidenreich, A.; Bahatt, D.; Ben-Horin, N.; Even, U.; Jortner, J. *J. Chem. Phys*. **1994**, *100*, 6300.
(11) Schmidt, M.; Le Calvè, J.; Mons, M. *J. Chem. Phys.* **1993**, *98*, 6102 and references therein.
(12) Albertí, M.; Aguilar, A.; Lucas, J. M.; Laganà, A.; Pirani, F. *J. Phys. Chem. A.* **2007**, *111*, 1780.
(13) Vacek, J.; Komvicka. K; Hobza, P. *Chem. Phys. Lett*. **1994**, *220*, 85.
(14) Vacek, J.; Hobza, P. *J. Phys. Chem*. **1994**, *98*, 11034.
(15) Pirani, F.; Albertí, M.; Castro, A.; Moix, M.; Cappelletti, D. *Chem. Phys. Lett*. **2004**, *394*, 37.
(16) Albertí, M.; Castro, A.; Laganà, A.; Pirani, F.; Porrini, M.; Cappelletti, D. *Chem. Phys. Lett*. **2004**, *392*, 514.

(17) Ondrechen, J. M.; Berkovitch-Yellin, Z.; Jortner, J. *J. Am. Chem. Soc*. **1981**, *103*, 6586.
(18) Mons, M.; Courty, A.; M.; Le Calvè, J.; Piuzzi, F.; Dimicoli, I. *J. Chem. Phys.* **1997**, *106*, 1676.
(19) Easter, D. C.; Bailey, L.; Mellot, J.; Tirres, M.; Weiss, T. *J. Chem. Phys*. **1998**, *108*, 6135.
(20) Cabarcos, O. M.; Weinheimer, J. C.; Lisy, J. M. *J. Chem. Phys.* **1998**, *108*, 5151.
(21) Cabarcos, O. M.; Weinheimer, J. C.; Lisy, J. M. *J. Chem. Phys.* **1999**, *110*, 8429.
(22) Le, Barbu, K.; Schiedt, J.; Weinkaut, R.; Schlag, E. W.; Nilles, J. M.; Xu, S. J.; Thomas, O. C.; Bowen, K. H. *J. Chem. Phys*. **2002**, *116*, 9663.
(23) Kumpf, R. A.; Dougherty, D. A. *Science* **1993**, *261*, 1708.
(24) Ma, J. C.; Dougherty, D. A. *Chem. Rev.* **1997**, *97*, 1303.
(25) Dougherty, D. A. *Science* **1996**, *271*, 163.
(26) Lee, J. I.; Sperry, D. C.; Farrar, J. M. *J. Chem. Phys.* **2001**, *114*, 6180.
(27) Morais-Cabral, J. H.; Zhou, Y.; MacKinnon, R. *Nature* **2001**, *414*, 37.
(28) Heginbotham, L.; MacKinnon, R. *Neuron* **1992**, *8*, 483.
(29) Albertí, M.; Aguilar, A.; Lucas, J. M.; Pirani, F.; Cappelletti, D.; Coletti, C.; Re, N. *J. Phys. Chem. A* **2006**, *110*, 9002.
(30) Albertí, M.; Castro, A.; Laganà, A.; Moix. M.; Pirani, F.; Cappelletti, D. *J. Phys. Chem. A* **2005**, *109*, 2906.
(31) Albertí, M.; Aguilar, A.; Lucas, J. M.; Cappelletti, D.; Laganà, A.; Pirani, F. *Chem. Phys.* **2006**, *328*, 221.
(32) Albertí, M.; Castro, A.; Laganà, A.; Moix. M.; Pirani, F.; Cappelletti, D. *Eur. Phys. J. C* **2006**, *38*, 185.
(33) Aguilar, A.; Albertí, M.; Laganà, A.; Pacifici, L. *Chem. Phys.* **2006**, *327*, 105.
(34) Dullweber, A.; Hodges, M. P.; Wales, D. J. *J. Chem. Phys.* **1997**, *106*, 1530.
(35) http://www.cse.clrc.ac.uk/ccg/software/DL_POLY/index.shtml.